Adhesion, Inelastic Contact Behaviour and Simulation of Shear Dynamics of Ultrafine Cohesive Powder

R. Tykhoniuk, J. Tomas
Dept. of Mech. Process Eng., Otto-von-Guericke University of Magdeburg, Universitätsplatz 2, D - 39106 Magdeburg, Germany

S. Luding
Particle Technology, DelftChemTech, TU Delft, Julianalaan 136, NL-2628 BL Delft, The Netherlands

M. Kappl, L. Heim, H.-J. Butt
MPI for Polymer Research, Ackermannweg 10, 55128 Mainz, Germany

ABSTRACT: Studies on the adhesion mechanics of particles give better physical understanding of essential constitutive functions of a cohesive powder "continuum". The discrete element method (DEM) allows us to consider in detail the contact and adhesion forces within force and momentum balance for each particle in a sheared particle packing. The introduction of irreversible inelastic contact flattening by the model, "stiff particles with soft contacts", is essential to describe the increase of adhesion force, i.e. of the van der Waals forces during preconsolidation. The history dependent dynamic behaviour of cohesive powder flow can be "microscopically" investigated and understood. Using a model for elastic-plastic contact behaviour between ultrafine particles (about 1 μm), steady-state flow, incipient yielding, dilatancy and consolidation of TiO_2 powder will be presented. Dynamic formation of a shear zone is also shown and compared to experiments in a standard Jenike shear cell.

1 INTRODUCTION

The well-known flow problems of cohesive particulate solids in storage and transportation containers, conveyors or process apparatuses include bridging, channelling, segregation, flooding, avalanching etc. In addition, the insufficient apparatuses and system reliability of solid processing plants are also related to flow problems. Taking into account this list of selected technical problems and hazards, this motivates us to deal with the fundamentals of cohesive powder consolidation and flow behaviour, i.e. to develop a reasonable combination of particle and continuum mechanics. The goal of the present work is to build a numerical bridge between the microscopic particle properties based on the atomic force microscope (AFM) measurements, theoretical models of elastic-plastic contact behaviour and the macroscopic powder flow behaviour of cohesive powders.

Continuum mechanical models and appropriate measuring methods were successfully applied to describe the flow behaviour of cohesive powders, as well as for practical design of process apparatus, e.g. silos. However, the essential constitutive functions of the powder "continuum" can be better described and understood with the help of particle mechanics (Tomas 2001). The Discrete Element Method (DEM) (Cundall 1992) is an alternative solution, which allows us to take into account the contact and, what is especially important in our case, adhesion forces and introduce them into the equations of motion of the particles. By this sophisticated method, the dynamic behaviour of cohesive powders can be studied and understood "microscopically".

Combining the theoretical background and macroscopic shear tests of cohesive powders as well as the microscopic AFM measurements of the particle interaction forces (Butt 1995), see also the parallel paper of these proceedings (Kappl 2005), it becomes possible to develop an appropriate contact constitutive model to describe the deformation behaviour of ultrafine, cohesive frictional particles. In this context, to simulate efficiently the shear dynamics of cohesive powders the implementation of an irreversible inelastic contact flattening, which is an essential element and physical reason for the load-dependent increase of the adhesion force, is of vital importance. There exists a realistic and flexible microscopic model for contact laws with elastic, plastic, and adhesion forces, as based on macroscopic observations from bulk experiments (Tomas 2001, Tomas 2002). The model in a simplified form is applied to the Jenike shear test as well as a biaxial shear box, in order to find out the relationships between the mechanical parameters of a single particle on a microscopic level and flow parameters of the powder continuum on the macroscopic level.

2 ADHESION AND INELASTIC CONTACT BEHAVIOUR

In terms of particle technology, powder processing and handling, the consolidation and non-rapid flow of dry, ultrafine and cohesive powders (particle diameter $d < 10$ μm) can be explained by the load-history dependent adhesion forces at particle contacts. Here we intend to focus on a characteristic soft

contact of two isotropic, stiff, linear elastic, smooth, spherical particles. Thus, the soft or compliant contact displacement is assumed to be small ($h_K/d << 1$) compared to the diameter of the stiff particles. The contact area consists of a representative number of molecules. Hence, continuum approaches are only used here to describe the force-displacement behaviour in terms of nanomechanics. The microscopic particle shape remains invariant during the dynamic stressing and contact deformation at this nanoscale. In powder processing, these particles are manufactured from uniform material in the bulk phase. These prerequisites are assumed to be suitable for the mechanics of dry particle contacts in many cases of industrial practice.

Here we introduce the constitutive model of Luding (Luding 2003) to be used in the numerical simulations since realistic and rather complicated contact model presented by Tomas (Tomas 2001), is very machine time spending to be implemented in the simulation software at present, Figure 1. That is why for the simulations we use the simplified contact law developed by Luding (Figure 1).

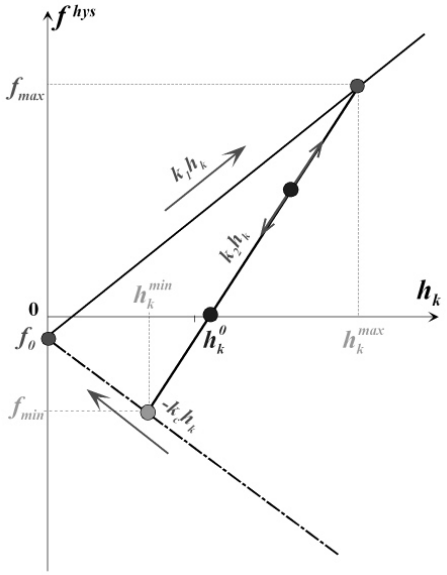

Figure 1. Linearized force displacement contact law

At the begin or end of the contact, i.e. when the contact deformation or particle-particle overlap is equal to 0, interaction between the particles starts from a predefined adhesion level ($-f_0$, here attractive forces are negative). The normal force then goes along the linear plastic yield limit with stiffness k_1, that takes care of a "perfect" plastic repulsion, considering also a linear dashpot that accounts for dissipation during contact. Inelastic deformation at the contact level is added by a linear spring, with a larger stiffness k_2 for unloading and reloading, so that the stiffness increases. The variable adhesion force (or cohesion on a microlevel) between the particles comes into the model by a "cohesive stiffness" k_c, which allows for changing the attractive forces up to a maximal attractive force f_{min} (per absolute value). One should notice also the force equilibrium state at a non-zero contact deformation of h_k^0. Cast into an equation, the normal force is:

$$f_n^{hys} = \begin{cases} k_1 h_k - f_0 & \text{for loading} \\ k_2 \left(h_k - h_k^0\right) & \text{for un-/reloading} \\ -k_c h_k - f_0 & \text{for unloading} \end{cases} \qquad (1)$$

The tangential force involves dissipation due to Coulomb friction, but also some tangential elasticity that allows for stick-slip behaviour on the contact level, see David et al. (David 2005) in this book.

3 SIMULATIONS

One possibility to gain insight about the material behaviour of a granular packing is to perform elementary tests in the laboratory. Here, we choose as alternative the simulation with the discrete element model (D'Addetta 2002, Kruyt 2001, Luding 2001, Oda 2000, Tykhoniuk 2004).

The discrete (or distinct) element solution scheme assumes each of its constituents as the separate entity. Mechanical behaviour of a system, containing of, in general, randomly shaped particles can be simulated by a generalized particle flow model. The particles displace independently from each other and interact only at contacts or with interfaces (walls). If the particles are assumed to be rigid, and the behaviour of the contacts is characterized using a soft contact approach, then the mechanical behaviour of such a system is described in terms of the movement of each particle and the inter-particle forces acting at each contact point. Newton's laws of motion for the translational and rotational degrees of freedom give the fundamental relationship between particle motion and the forces and moments that induce them:

$$m_i \frac{d^2}{dt^2} \vec{r}_i = \vec{f}_i + m_i \vec{g} \qquad \text{and} \qquad I_i \frac{d}{dt} \vec{\omega}_i = \vec{t}_i \qquad (2)$$

with the gravitational acceleration $\vec{g}$, mass m_i of the particle, its position $\vec{r}_i$, the total force $\vec{f}_i$, acting on it due to contacts with other particles or with the walls, its moment of inertia I_i, its angular velocity $\vec{\omega}_i$, and the total torque $\vec{t}_i$.

The first simulations are performed only with the linear adhesion contact law, which was originally implemented into the software (PFC2D, Itasca Inc.). For convenience, a constant adhesion force of 1-10 mN (0.1-1% of average contact forces of loading) was used to approximate the load-history dependent pull-off force (Tomas 2001). Then a series of simulations is done applying the more general dissipative contact model for adhesive particles (Figure 1), and the comparison is made.

The classical translational shear cell, developed by Jenike (Jenike 1964), is modelled (Figure 2). Considering a suitable CPU-time for the simulations one should imagine that we simulate here only a small two-dimensional (2D) element from the real shear cell. Figure 2 shows the model for 2000 titanium dioxide particles with diameter of about (3±0,5) µm. The upper wall (shear lid) is stress controlled, i.e. when the reaction force F_N changes because of the particle reorganization, the height of the shear lid is changed as well. The predefined normal stress is $\sigma=F_N/A$ (A is replaced by d_Z in the 2D case). The horizontal shear rate of the upper part of the cell is preset, i.e. the upper ring is strain driven. As the direct response, the corresponding values of the reaction force are obtained, which acts on the lateral walls. Furthermore, the corresponding shear stresses $\tau=F_S/A$ are calculated enabling in this way to find the flow parameters of the simulated model powder. The shear rate applied here is about 1-4 mm/min (similar to the one used in the Jenike shear cell in laboratory tests).

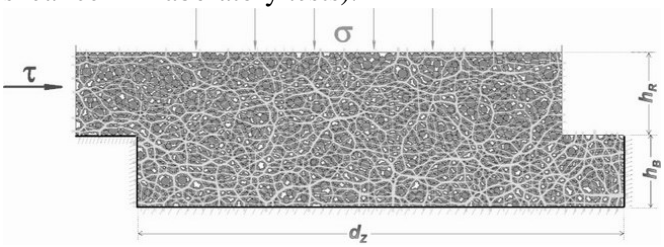

Figure 2. The shear cell model system for the simulations (lines in the particle system show the initial contact forces, with line thickness proportional to force)

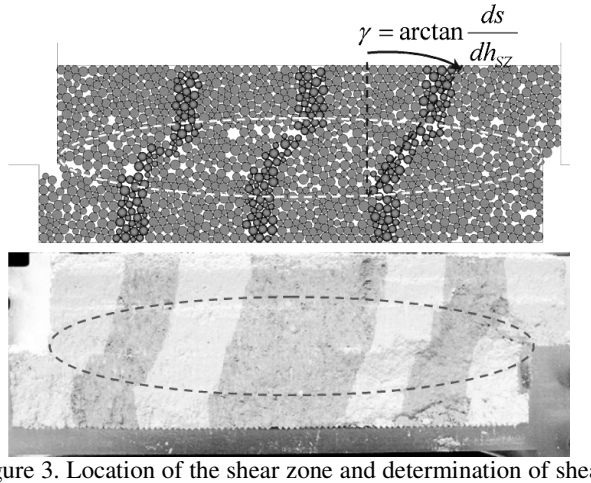

Figure 3. Location of the shear zone and determination of shear distortion (top: simulation, bottom: experiment)

Figure 3 presents the whole particle system after shearing both for the simulations and the experiment (bottom). The shear zone and the angle γ, the so-called shear distortion are clearly recognised here. The angle γ is defined as a function of the shear displacements and the shear zone height h_{SZ}.

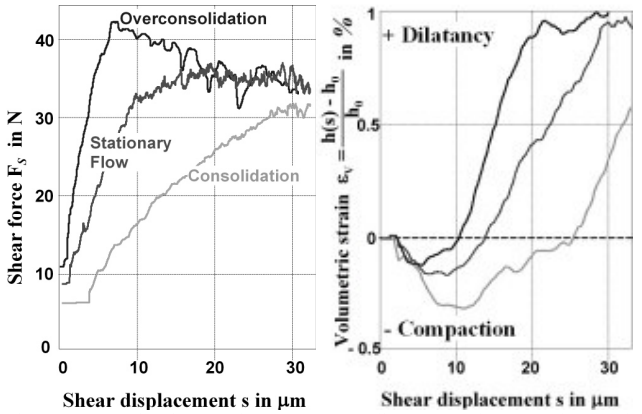

Figure 4. Left: force-displacement diagram; right: volumetric strain for different initial porosity values

Figure 4 shows the force-displacement diagram (left) and the volumetric strain (right) at the constant normal stress of $\sigma_N=3\ kPa$ for three different values of initial porosity $\varepsilon=1-\rho_b/\rho_s$ (where ρ_b is the bulk material density, and ρ_s the solid density), i.e. three so-called preshear tests. The upper curves in both graphs are obtained at a two-dimensional porosity of the particle system of $\varepsilon_{2D}=0.16$. The typical behaviour of the overconsolidated powder is observed in this case achieving the peak force value along with the first-stage compaction at the beginning and tending to the steady state flow later on. The middle curves at $\varepsilon_{2D}=0.18$ show almost ideal steady-state flow with the remark that the volumetric strain is coming to relatively stable state only at the end of the shear process, which is not in agreement with the theoretical expectations. The fluctuations of the shear force can be explained by means of the temporary and local shear-thickening and shear-thinning processes. The lower curves correspond to $\varepsilon_{2D}=0.20$ and show the behaviour of an underconsolidated powder.

Figure 5 shows the comparison of yield locus calculated from the Jenike shear cell experiments with the simulated yield loci obtained applying the different contact laws with somewhat different parameters (see Table 1). The experimental data (the upper line) show the internal friction angle of the powder continuum to be equal to $\varphi_i = 26°$, and the macroscopic cohesion $\tau_c = 3{,}09\ kPa$. The lower line is the result of the simulated shear test, where the microscopic interactions between the particles are described using the so-called linear-spring-dashpot contact model (Hook's law with microscopic dissipation, see Table 1, Simulation 1) in normal direction extended only by the constant adhesion force between the particles in contact (see $-f_0$ on the Figure 1). And, finally, the two lines in the middle (Table 1, Simulation 2 and 3) are obtained by means of applying the implemented elastic-plastic microscopic contact model with variable adhesion (Figure 1), though the upper one (Table 1, Simulation 3) from the two with higher "microscopic cohesive stiffness" (k_c on the

Figure 1), giving as the macroscopic result the internal friction angle of $\varphi_i = 20°$, and the cohesion of $\tau_c = 1{,}13\ kPa$. As one can see, direct quantitative comparison of the simulated data with experiments does not still give the satisfactory agreement. However, the implemented "cohesive" contact model shows a "positive" influence on the macroscopic flow behaviour of a consolidated powder bed. Very important result is the fact that the macroscopic cohesion τ_c can be related to the maximal microscopic attractive force f_{min}, see Kappl 2005.

Table 1. Contact model properties used in the simulations

Simulation	Contact model	Stiffness k_1	k_2	k_c
1	Hook	10^8 N/m	10^8 N/m	10^8 N/m
2	Cohesive	10^8 N/m	$2 \cdot 10^8$ N/m	$2 \cdot 10^8$ N/m
3	Cohesive	10^8 N/m	$2 \cdot 10^8$ N/m	$8 \cdot 10^8$ N/m

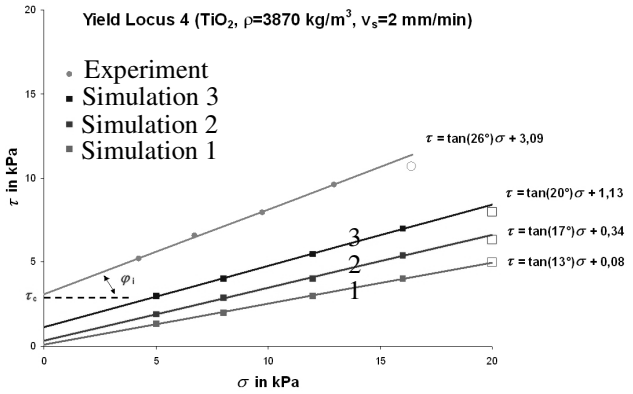

Figure 5. Shear stress - normal stress diagram of yield locus 4 of model material (TiO_2) for experiment and different microscopic force-displacement laws (linear and "cohesive")

4 CONCLUSIONS

In summary, a set of DEM simulations based on different contact constitutive models are presented, and several macroscopic material parameters like, e.g., the friction angle, were extracted from the simulation data with chosen microscopic input parameters. Altogether this is a first step of a micro-modelling approach for cohesive frictional powders by means of going the long way from a measurement of ultrafine single particles, and implementing the complex microscopic contact constitutive laws for the contacts between the particles, up to the shear dynamics of big particle systems finding out in this way the macroscopic flow parameters of bulk materials.

So far, good qualitative agreement of the simulations with experiments is reached. The implemented "cohesive" contact model shows a "positive" influence on the macroscopic flow behaviour of a consolidated powder bed. The model shows to be capable of simulating the cohesive properties of a material with variable adhesion (pull-off) force depending among others on the preconsolidation history of every inelastic particle contact deformation. An important result is the fact that the macroscopic cohesion can be related to the maximum microscopic attractive force.

Further material parameters have to be identified, and also the role of particle rotations is an open issue, as related to micro-polar constitutive models. In both simulations and experiments, rotations are active in the shear band where the rotational degree of freedom is activated. The corresponding parameter identification and the micro-macro-transition for anisotropic micro-polar continuum models (Tejchman 1993) is challenge for the future, like the implementation and simulation of experimentally determined force-laws in three-dimensional systems.

5 ACKNOWLEDGEMENT

The authors acknowledge the financial support from the German Research Foundation (DFG).

REFERENCES

Butt, H.-J., Jaschke, M. & Ducker, W.A. 1995. Measuring surface forces in aqueous solution with the atomic force microscope. *Bioelectrochem. Bioenerg.* 381, 91-201.

Cundall, P. A & Hart, R. D. 1992. Numerical modelling of diskotinua. 1st US Conference on DEM. *Eng. Comput.* 9, 101-113.

D'Addetta, G. A., Kun, F. & Ramm, E. 2002. On the application of a discrete model to the fracture process of cohesive granular materials. *Granular Matter* 4 (2), 77-90.

David, C.T., Rojo, R.G., Herrmann, H.J. & Luding, S. Hysteresis and creep in powders and grains, *Proc. of Powders&Grains'2005.*

Jenike, A.W. 1964. Storage and flow of solids. *Eng. Exp. Station*, Bull. No. 123, Univ. Utah.

Kappl, M., Heim, L., Butt, H.-J., Luding, S., Tykhoniuk, R. & Tomas, J. 2005. From grains to powders: from single particle contact mechanics measurements to bulk powder properties, *Proc. of Powders&Grains'2005.*

Kruyt, N. P. & Rothenburg, L. 2001: Statistics of the elastic behaviour of granular materials. *Int. J. of Solids and Structures* 38, 4879-4899.

Luding, S., Lätzel, M., Volk, W., Diebels, S. & Herrmann, H.J. 2001. From discrete element simulations to a continuum model. *Comp. Meth. Appl. Mech. Engng.* 191, 21-28.

Luding, S., Tykhoniuk, R. & Tomas, J. 2003. Anisotropic material behaviour in dense, cohesive powders. *Chem. Eng. Tech.* 26 (12), 1229-1232.

Oda, M. & Iwashita, K. 2000. Study on couple stress and shear band development in granular media based on numerical simulation analyses, *Int. J. of Eng. Sci.* 38, 1713-1740.

Tomas, J. 2001. Assessment of mechanical properties of cohesive particulate solids – part 1: particle contact constitutive model. *Particulate Science & Technology* 19-2, 95-110.

Tomas, J. 2002. Zur Mechanik trockener kohäsiver Schüttgüter. *Schüttgut* 8-6, 522-537.

J. Tejchman & W. Wu 1993. Numerical study on patterning of shear bands in a Cosserat continuum. *Acta Mechanica 99*: 61-74.

Tykhoniuk, R., Luding, S. & Tomas, J. 2004. Simulation der Scherdynamik Kohäsiver Pulver, *Chemie Ingenieur Technik* 76, No. 1-2, 59-62.